

Influence of Damping Constant on Writability in Heated-Dot Magnetic Recording

T. Kobayashi, I. Tagawa*, and Y. Nakatani**

Graduate School of Engineering, Mie Univ., 1577 Kurimamachiya-cho, Tsu 514-8507, Japan

*Electrical and Electronic Engineering, Tohoku Institute of Technology, 35-1 Yagiyama-Kasumicho, Sendai 982-8577, Japan

**Graduate School of Informatics and Engineering, Univ. of Electro-Communications, 1-5-1 Chofugaoka, Chofu 182-8585, Japan

We discuss the influence of the damping constant α on writability in heated-dot magnetic recording using our stochastic calculation employing the Néel-Arrhenius model with a Stoner-Wohlfarth dot, since the duration for the non-Néel-Arrhenius type is very short in the writing time and most of the writing time is the Néel-Arrhenius type. The bit error rate is calculated and the result is analyzed using the mean magnetization reversal numbers per unit time N_+ and N_- for the magnetization reversal in the direction opposite to the recording direction and in the recording direction, respectively. The writing improves as the N_+ value decreases and the N_- value increases. The N_+ and N_- values decrease as the α value decreases, since the attempt frequency is approximately proportional to α . The writing time when the N_- value is large is rather short compared with the writing time determined by the writing field. Therefore, a magnetization reversal time that is much shorter than the writing time is needed to write data. The $1/N_+$ value represents the stochastic magnetization reversal time under thermal agitation, and the $1/N_-$ value is inversely proportional to α . Although the N_+ value becomes small, a small α value is disadvantageous to writing.

Key words: HDMR, Gilbert damping constant, stochastic calculation, micromagnetic simulation, bit error rate, reversal number, reversal time

1. Introduction

Many magnetic recording methods have been proposed to solve the trilemma problem¹⁾ of conventional magnetic recording (CMR) on granular media. These methods include shingled magnetic recording (SMR), microwave-assisted magnetic recording (MAMR), heat-assisted magnetic recording (HAMR), bit patterned media (BPM), heated-dot magnetic recording (HDMR), namely HAMR on BPM, and three-dimensional magnetic recording (3D MR).

Akagi *et al.* reported writability in HDMR²⁾ and 3D HDMR^{3,4)} employing micromagnetic simulation. They assumed the medium material to be FePt. However, the anisotropy constant K_u was smaller than that of bulk FePt.

We have discussed the influence of K_u on writability in HDMR⁵⁾ employing our stochastic calculation using the Néel-Arrhenius model with a Stoner-Wohlfarth dot. We explained why HDMR with a small K_u exhibits good writability using the mean magnetization reversal number per unit time N_+ in the opposite direction to the recording direction and the N_- value in the recording direction during writing. When we choose a small K_u value, the N_+ value becomes negligible. Furthermore, the duration where the N_- value is large becomes longer. These are advantageous as regards writability.

A feature of our stochastic calculation is that it is easy to grasp the physical implication of HAMR writing

including HDMR.

The magnetization precession, namely the damping constant is a common problem for HAMR and HDMR. We have already discussed the influence of the damping constant on writability for media with relatively small and large anisotropy constants in HAMR⁶⁾ employing our stochastic and micromagnetic calculations. However, the discussion lacked the temperature dependence of an attempt frequency, namely the perspective provided by the N_{\pm} values. Using the N_{\pm} values, we can understand the magnetization motion during writing in detail.

In this paper, we discuss the influence of the damping constant on writability for a medium with a large anisotropy constant in 4 Tbps shingled HDMR, employing our stochastic calculation using the N_{\pm} values. This condition simplifies the analysis of the writing process, since 1 bit consists of 1 dot for HDMR and erasure-after-write can be ignored for a medium with a large anisotropy constant⁵⁾. We confirm the stochastic calculation result by employing a micromagnetic simulation.

2. Calculation Conditions and Method

2.1 Dot arrangement and medium structure

Figure 1 shows the dot arrangement and medium structure in 4 Tbps HDMR where D_x , D_y , and h are the dot sizes for the down-track x and cross-track y directions, and the dot height, respectively. The z direction is film normal. The bit length D_B and track width D_T are both 12.7 nm. We assume that the mean dot size D_m and mean dot spacing Δ_D are the same for

Corresponding author: T. Kobayashi (e-mail: kobayashi@phen.mie-u.ac.jp).

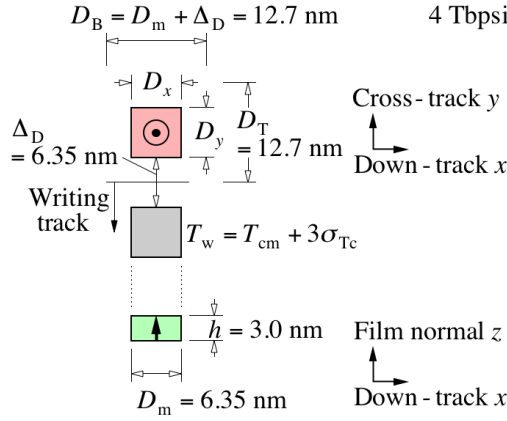


Fig. 1 Dot arrangement and medium structure.

both the down-track and cross-track directions, namely $D_m = \Delta_D = 6.35$ nm.

There are two cases as regards the dot sizes D_x and D_y depending on the dot manufacturing method. In one, the D_x and D_y sizes are the same, and the $D_x = D_y$ size fluctuates. In the other case, the D_x and D_y sizes fluctuate independently. We examined the $D_x = D_y$ case. We generated a random number $D_x = D_y$ that had a log-normal distribution with a standard deviation σ_D . We used a σ_D/D_m value of 15 %.

2.2 Temperature profile and writing field

The writing temperature T_w for the dot was assumed to be

$$T_w = T_{cm} + 3\sigma_{Tc}, \quad (1)$$

as shown in Fig. 1, after taking account of the Curie temperature T_c variation, where T_{cm} and σ_{Tc} are the mean Curie temperature and the standard deviation of T_{cm} , respectively. The T_c distribution was assumed to be normal. Based on this assumption, 99.9 % of the dots in the writing track are heated to above their T_c values during the writing period. We used T_{cm} and σ_{Tc}/T_{cm} values of 750 K and 2 %, respectively.

For simplicity, we used a thermal gradient $\partial T/\partial y$ of 14 K/nm in the cross-track direction and assumed it to be constant anywhere for adjacent track interference (ATI). A constant thermal gradient $\partial T/\partial x$ of 14 K/nm in the down-track direction was also used for writability.

The writing field H_w was assumed to be spatially uniform, the direction to be perpendicular to the medium plane, and the rise time to be zero.

2.3 Magnetic properties

The temperature T dependence of the medium magnetization M_s was calculated by employing mean field analysis⁷⁾ for $(\text{Fe}_{0.5}\text{Pt}_{0.5})_{1-c}\text{Cu}_c$, and that of the K_u value was assumed to be proportional to $M_s^{2.8}$. $M_s(T_c = 770 \text{ K}, T = 300 \text{ K}) = 1000 \text{ emu/cm}^3$ was assumed for FePt. Based on this assumption, the M_s value can be calculated for all values of T_c and T .

Since each dot has a T_c variation, the T_c value of each

Table 1 Calculation conditions.

Recording density (Tbpsi)	4
Bit length D_B (nm)	12.7
Track width D_T (nm)	12.7
Mean dot size D_m (nm)	6.35
Standard deviation σ_D / D_m (%)	15
Dot height h (nm)	3.0
Mean dot spacing Δ_D (nm)	6.35
Mean Curie temperature T_{cm} (K)	750
Standard deviation σ_{Tc} / T_{cm} (%)	2
Thermal gradient $\partial T / \partial x$ (K / nm)	14
Linear velocity (m / s)	10
Storage temperature (K) for 10 years of archiving	350
Thermal gradient $\partial T / \partial y$ (K / nm) for ATI	14
Exposure field (kOe) for ATI	10
Exposure time (ns) for ATI	1

dot was adjusted by changing the Cu composition c for $(\text{Fe}_{0.5}\text{Pt}_{0.5})_{1-c}\text{Cu}_c$.

We used a K_u value of 51 Merg/cm³ and an anisotropy field H_k of 107 kOe at a readout temperature of 330 K.

When we choose an h value, 10 years of archiving, ATI, and writability must be dealt with simultaneously, since they are in a trade-off relationship. The calculation conditions are summarized in Table 1. We assumed the storage temperature to be 350 K for 10 years of archiving, for which we took a certain margin into account. We used an exposure field of 10 kOe and a time of 1 ns for ATI. We fixed the h value at 3.0 nm, taking account of 10 years of archiving and ATI. The limiting factor is 10 years of archiving and the damping constant has little effect on 10 years of archiving⁹⁾. The linear velocity v was 10 m/s.

2.4 Stochastic calculation method

The information stability for 10 years of archiving has been discussed employing the Néel-Arrhenius model with a Stoner-Wohlfarth grain or dot¹⁾. The attempt period $1/f_a$ has a value of picoseconds for FePt in HAMR. Since the magnetization direction attempts to reverse with a certain probability at each attempt period, the information stability for 10 years of archiving is extrapolated as a stack of phenomena in picoseconds. Therefore, the Néel-Arrhenius model is valid for any time from the order of a picosecond to more than 10 years. The Néel-Arrhenius model is also valid on condition that the writing field is smaller than the anisotropy field of the recording media.

Figure 2 shows (a) the temperature dependence of K_u and (b) the time dependence of the effective anisotropy field H_{keff} for a medium with T_{cm} , which was calculated from Eq. (11) described below. The medium temperature is also shown. At a time of zero, the medium temperature is assumed to be T_{cm} and the H_w direction changes

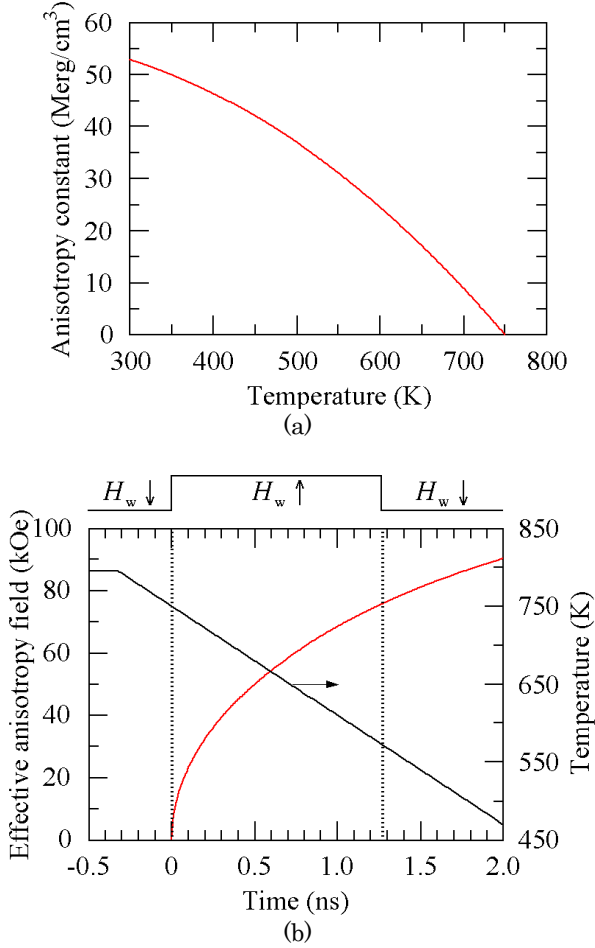


Fig. 2 (a) temperature dependence of anisotropy constant K_u and (b) time dependence of effective anisotropy field H_{keff} and medium temperature.

from downward to upward, and at a time of 1.27 ns it changes from upward to downward. The writing time defined by H_w , namely the field writing time is 1.27 ns. The time is advanced by $\sigma_{Tc}/((\partial T/\partial x) \cdot v)$ for a medium with $T_{cm} + \sigma_{Tc}$ and delayed for a medium with $T_{cm} - \sigma_{Tc}$. When $|H_w| > H_{keff}$, the magnetization reversal is the non-Néel-Arrhenius type. The duration for the non-Néel-Arrhenius type is very short, and most of the field writing time is the Néel-Arrhenius type where $|H_w| < H_{keff}$. In HAMR including HDMR, stochastic magnetization reversal under thermal agitation is dominant even for writability. Therefore, we have been applying the Néel-Arrhenius model to phenomena with a short time and examined ATI⁹⁾ and writability⁵⁾.

The mean magnetization reversal number per unit time N is expressed as

$$N = f_\alpha \exp(-K_\beta), \quad (2)$$

employing the Néel-Arrhenius model with a Stoner-Wohlfarth grain or dot, where f_α is the attempt frequency¹⁰⁾ and K_β is the thermal stability factor. The f_α value gives an attempt number per unit time for magnetization reversal, and the Boltzmann factor $\exp(-K_\beta)$ is interpreted as the probability of

magnetization reversal.

When the $|H_w|$ value is less than H_k , $f_\alpha \equiv f_{\alpha+}$, $K_\beta \equiv K_{\beta+}$, and $N \equiv N_+$ are given by

$$f_{\alpha+} = \frac{\gamma\alpha}{1+\alpha^2} \sqrt{\frac{M_s H_k^3 V}{2\pi kT}} \left(1 - \left(\frac{|H_w|}{H_k}\right)^2\right) \left(1 + \frac{|H_w|}{H_k}\right), \quad (3)$$

$$K_{\beta+} = \frac{K_u V}{kT} \left(1 + \frac{|H_w|}{H_k}\right)^2, \text{ and} \quad (4)$$

$$N_+ = f_{\alpha+} \exp(-K_{\beta+}), \quad (5)$$

respectively, for magnetization reversal in the opposite direction to the recording direction, where γ , α , V , and k are the gyromagnetic ratio, Gilbert damping constant, dot volume $V = D_x D_y \times h$, and Boltzmann constant, respectively. We used a γ value of $1.76 \times 10^7 \text{ rad s}^{-1} \text{ Oe}^{-1}$. For magnetization reversal in the recording direction, $f_\alpha \equiv f_{\alpha-}$, $K_\beta \equiv K_{\beta-}$, and $N \equiv N_-$ are given by

$$f_{\alpha-} = \frac{\gamma\alpha}{1+\alpha^2} \sqrt{\frac{M_s H_k^3 V}{2\pi kT}} \left(1 - \left(\frac{|H_w|}{H_k}\right)^2\right) \left(1 - \frac{|H_w|}{H_k}\right), \quad (6)$$

$$K_{\beta-} = \frac{K_u V}{kT} \left(1 - \frac{|H_w|}{H_k}\right)^2, \text{ and} \quad (7)$$

$$N_- = f_{\alpha-} \exp(-K_{\beta-}), \quad (8)$$

respectively.

In our stochastic calculation, we used the effective anisotropy constant K_{ueff} instead of K_u and the effective anisotropy field H_{keff} instead of H_k , taking account of the shape anisotropy¹¹⁾, as

$$K_{ueff} = K_u + \frac{(4\pi - 3N_z)M_s^2}{4}, \quad (9)$$

$$N_z = 8 \arctan\left(\frac{D_x D_y}{h\sqrt{D_x^2 + D_y^2 + h^2}}\right), \text{ and} \quad (10)$$

$$H_{keff} = \frac{2K_{ueff}}{M_s}. \quad (11)$$

The magnetostatic field from surrounding dots was ignored.

When calculating the information stability for 10 years of archiving ($|H_w| = 0$) or ATI, we used Eqs. (6) - (8) modified by Eqs. (9) - (11), since the H_{keff} value is of course much larger than $|H_w|$. Although there is a period where $H_{keff} < |H_w|$ during writing, the duration is much short as shown in Fig. 2 (b). The factor $\sqrt{M_s H_k^3/T}$ in Eqs. (3) and (6) has a strong impact on the temperature dependence of $f_{\alpha\pm}$, and $(1 - (|H_w|/H_k)^2)(1 \pm |H_w|/H_k)$ is a weakly impacting factor since the H_k value is considerably larger than $|H_w|$ for most of the writing time. Although the $\sqrt{M_s H_k^3/T}$ value becomes zero at T_c , $(1 - (|H_w|/H_k)^2)(1 \pm |H_w|/H_k)$ reaches zero at a temperature where $H_k = |H_w|$. We employed the Néel-Arrhenius model for the entire field writing time. To

achieve this, we extended the $f_{\alpha\pm}$ formula to T_c as

$$f_{\alpha\pm} = \frac{\gamma\alpha}{1+\alpha^2} \sqrt{\frac{M_s H_{\text{keff}}^3 V}{2\pi k T}} \left(1 - \left(\frac{|H_w|}{H_{\text{const}}}\right)^2\right) \left(1 \pm \frac{|H_w|}{H_{\text{const}}}\right), \quad (12)$$

so that the $f_{\alpha\pm}$ value becomes zero at T_c where the positive and negative signs are in the same order. H_{const} in Eq. (12) is a fitting parameter for Eqs. (3) and (6) and we used a H_{const} value of 60 kOe. When $|H_w| > H_{\text{keff}}$, we assumed that

$$K_{\beta-} = 0. \quad (13)$$

The calculation procedure for the writing field dependence of the bit error rate (bER), namely writability, is described below. The dot temperature fell with time from T_c according to $\partial T/\partial x$ and v . The attempt times were calculated using $f_{\alpha\pm}$. The probabilities $\exp(-K_{\beta\pm})$ were calculated for every attempt time. The magnetization direction was determined by the Monte Carlo method for every attempt time. Then the bER value was obtained. The calculation detail has already been reported¹².

The bER in this paper is useful only for comparisons.

3. Calculation Results

3.1 Writing field dependence of bit error rate

Figure 3 (a) shows the writing field $|H_w|$ dependence of bER calculated employing our stochastic calculation. The bER value increases as the α value decreases.

We confirmed the result in Fig. 3 (a) by employing a micromagnetic simulation in which we solved the Landau-Lifshitz-Gilbert (LLG) equation. The LLG calculation method has already been reported in detail⁶. Figure 3 (b) shows the $|H_w|$ dependence of the signal to noise ratio (SNR) calculated employing a micromagnetic simulation, and Fig. 3 (c) shows the bER value in Fig. 3 (a) as a function of the SNR value in Fig. 3 (b). A good correlation can be seen between them. Therefore, our stochastic calculation in Fig. 3 (a) can almost entirely explain the result of the micromagnetic simulation in Fig. 3 (b).

We first discuss this result in terms of the attempt frequency in the Néel-Arrhenius model and the magnetization reversal time constant in the LLG equation.

Since the α value is considered to be smaller than 0.1, $f_{\alpha\pm}$ is almost proportional to α as shown in Eq. (12) since $\alpha/(1+\alpha^2) \approx \alpha$. This means that the attempt number for the magnetization reversal in the recording direction becomes smaller as the α value decreases. As a result, the bER value increases as the α value decreases.

On the other hand, the LLG equation can be solved for a single domain particle. When the initial magnetization and field directions are the z and $-z$ directions, respectively, and the magnetization direction is expressed in a polar coordinate, the magnetization

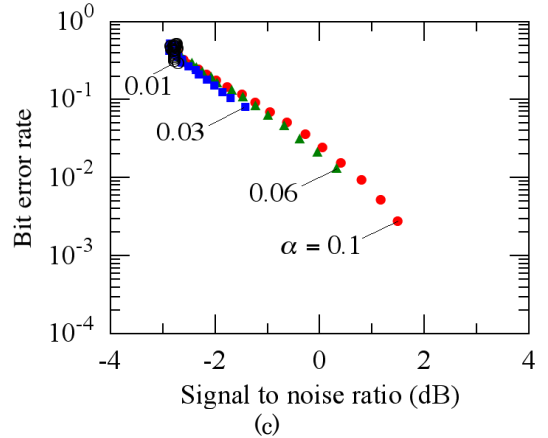
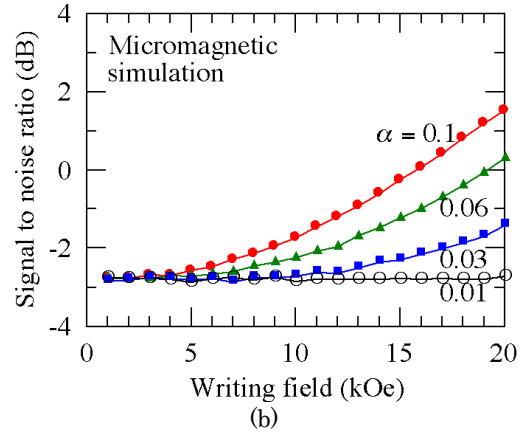
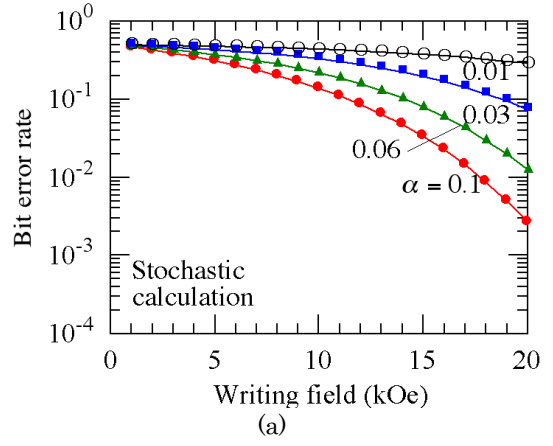


Fig. 3 Writing field $|H_w|$ dependence of (a) bit error rate (bER) calculated employing our stochastic calculation and (b) signal to noise ratio (SNR) calculated employing a micromagnetic simulation for various α values. (c) The bER value in (a) as a function of the SNR value in (b).

motion is given by

$$\phi = \omega t + \phi_0, \text{ and} \quad (14)$$

$$\theta = 2 \arctan \left(\tan \left(\frac{\theta_0}{2} \right) \exp \left(-\frac{t}{\tau} \right) \right), \quad (15)$$

as a function of time t where ϕ and θ are the azimuth

and polar angles, respectively¹³. ϕ_0 and θ_0 are the initial values at $t = 0$. ω represents the angular frequency when it is precessing around the field H , τ represents the magnetization reversal time constant in the field direction, and those are given by

$$\omega = \frac{\gamma H}{1 + \alpha^2}, \text{ and} \quad (16)$$

$$\tau = \frac{1}{\alpha \omega} = \frac{1 + \alpha^2}{\alpha} \cdot \frac{1}{\gamma H}. \quad (17)$$

Equation (17) includes a factor of $(1 + \alpha^2)/\alpha \approx 1/\alpha$. This means that the magnetization reversal time becomes longer as the α value decreases. If the magnetization reversal time is too long compared with the writing time, many errors occur. As a result, the bER value increases as the α value decreases.

3.2 N_+ value and magnetization motion

Next, we discuss the N_+ value, which is the mean magnetization reversal number per unit time in the opposite direction to the recording direction, and the corresponding magnetization motion.

The $N_+ = f_{\alpha+} \exp(-K_{\beta+})$ value as a function of time is shown in Fig. 4 for various α values where $|H_w| = 10$ kOe. As the N_+ value decreases, the writing improves, and the N_+ value decreases as the α value decreases since the $f_{\alpha+}$ value is proportional to $\alpha/(1 + \alpha^2) \approx \alpha$.

We also confirmed the meaning of N_+ in Fig. 4 by employing a micromagnetic simulator, EXAMAG LLG (Fujitsu Ltd.)¹⁴, in which the Landau-Lifshitz-Gilbert (LLG) equation is solved by the finite-element method. We added the equivalent field for the energy of the thermal agitation. The calculation step time was 10^{-16} s. We focused on the magnetization motion at 0.070 ns in Fig. 4, at which the N_- value for $\alpha = 0.1$ exhibits its maximum value as shown later in Fig. 6, and the temperature is 740 K. Figure 5 shows the time dependence of the magnetization z component M_z/M_s , which means the magnetization motion as a function of time. The initial magnetization and writing field

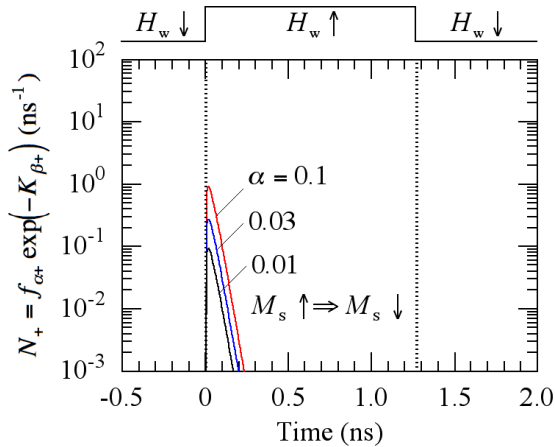


Fig. 4 Mean magnetization reversal number per nanosecond $N_+ = f_{\alpha+} \exp(-K_{\beta+})$ as a function of time for various α values where $|H_w| = 10$ kOe.

directions are the $-z$ and z directions, respectively. The dot size and magnetic property in Fig. 4 were the same as those in Fig. 5. The calculation temperature was constant at 740 K where $|H_w| = 10$ kOe and $H_{\text{keff}} = 19$ kOe.

Since the $N_+(740 \text{ K})$ value is 0.26 ns^{-1} for $\alpha = 0.1$, we can expect there to be 0.26 mean magnetization reversals in the opposite direction to the recording direction within 1 ns as shown in Fig. 4. As expected, several magnetization reversals can be observed within

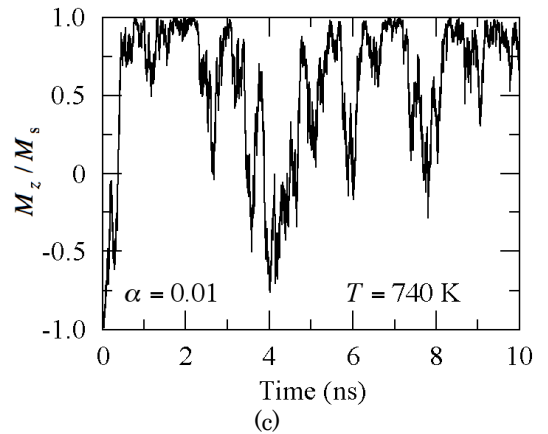
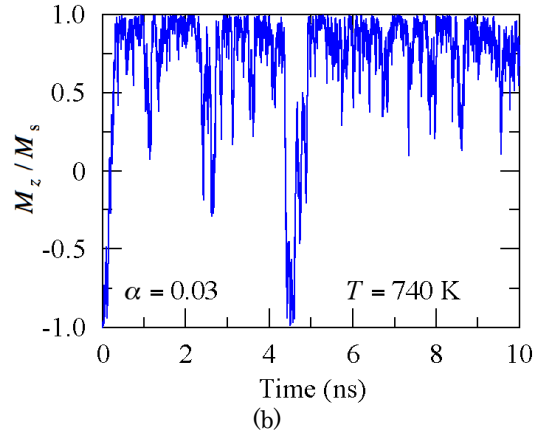
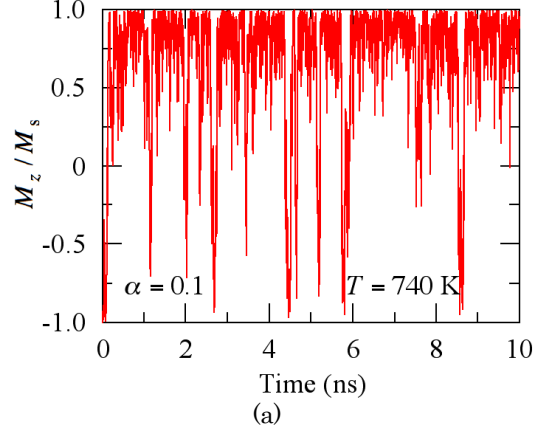


Fig. 5 Time dependence of magnetization z component M_z/M_s at 740 K (0.070 ns) for (a) $\alpha = 0.1$ ⁵, (b) $\alpha = 0.03$, and (c) $\alpha = 0.01$ where $|H_w| = 10$ kOe and $H_{\text{keff}} = 19$ kOe.

10 ns as shown in Fig. 5 (a), as already reported⁵). If we employ a definition stating that the magnetization is reversed when the M_z/M_s value falls below than -0.9 , the magnetization reversal number is 4 times for the example in Fig. 5 (a). This means that there is a situation where the magnetization reverses in the opposite direction to the recording direction. When (b) $\alpha = 0.03$, it is expected that there will be 0.78 mean magnetization reversals in the opposite direction to the recording direction within 10 ns since the $N_+(740\text{ K})$ value is 0.078 ns^{-1} . And one magnetization reversal can be seen in Fig. 5 (b). For (c) $\alpha = 0.01$, the $N_+(740\text{ K})$ value is 0.026 ns^{-1} , and the M_z/M_s value does not reach less than -0.9 within 10 ns for this example as shown in Fig. 5 (c).

The stochastic calculation result in terms of the N_+ value is consistent with that employing a micromagnetic simulation.

3.3 N_- value and magnetization motion

Finally, we discuss the N_- value and corresponding magnetization motion.

The N_- (ns^{-1}) value also decreases as the α value decreases as shown in Fig. 6. This means that the mean magnetization reversal number per nanosecond in the recording direction decreases as the α value decreases. The $N_- = f_{\alpha-} \exp(-K_{\beta-})$ value shows the maximum, since the $f_{\alpha-}$ value increases and the $\exp(-K_{\beta-})$ value decreases rapidly as the temperature decreases⁵.

We also focused on the magnetization motion at 0.070 ns in Fig. 6. Since the magnetization motion fluctuates with thermal energy, we calculated it using six different random seeds for $\alpha = 0.1$ as shown in Fig. 7 (a). In one case, the magnetization reverses rapidly, and in another case, slowly after time 0. Figure 7 (b) shows the mean magnetization $\langle M_z \rangle / M_s$ as a function of time for six different random seeds. The $\langle M_z \rangle / M_s$ reversal time defined by the time for $\langle M_z \rangle / M_s = 0$ is 0.094 ns, which can be compared to a $1/N_-(740\text{ K})$ value of 0.073 ns.

The writing time determined by the medium, where the $N_- = f_{\alpha-} \exp(-K_{\beta-})$ value is large, is rather short

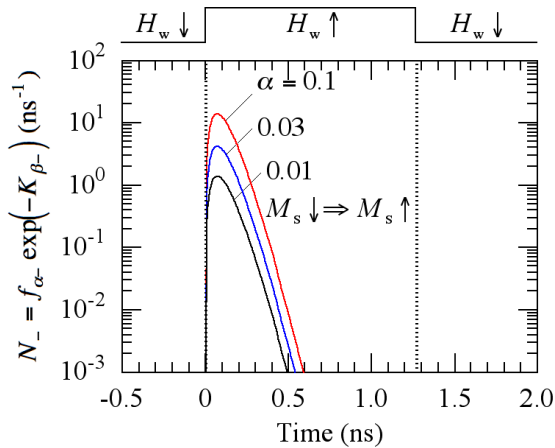


Fig. 6 Mean magnetization reversal number per nanosecond $N_- = f_{\alpha-} \exp(-K_{\beta-})$ as a function of time for various α values where $|H_w| = 10\text{ kOe}$.

compared with the field writing time as shown in Fig. 6, since the $\exp(-K_{\beta-})$ value decreases rapidly with time.

Although the temperature was constant for the calculation in Fig. 7, the temperature decreases with time during writing as shown in Fig. 2. For example, at a time of 0.59 ns, which corresponds to a temperature of

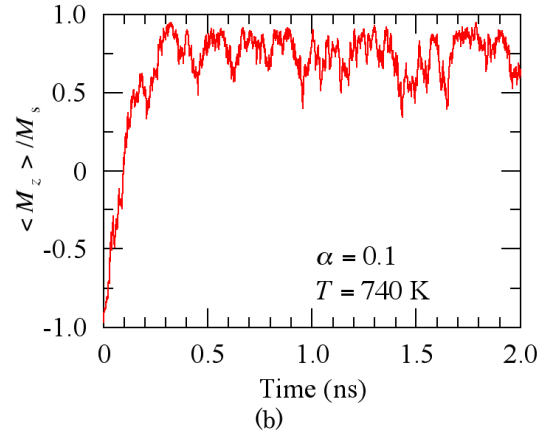
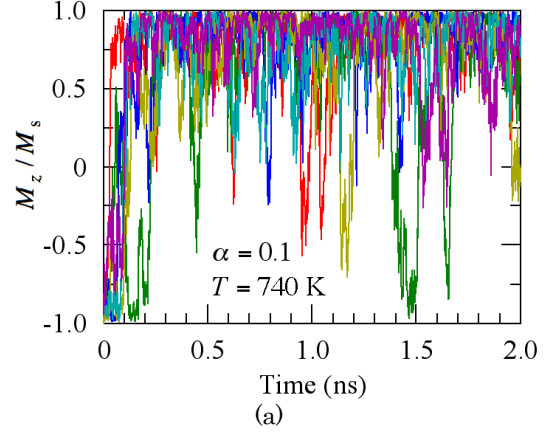


Fig. 7 (a) Time dependence of magnetization z component M_z/M_s calculated using six different random seeds at 740 K (0.070 ns) for $\alpha = 0.1$ where $|H_w| = 10\text{ kOe}$ and $H_{\text{keff}} = 19\text{ kOe}$. (b) Mean magnetization $\langle M_z \rangle / M_s$ as a function of time.

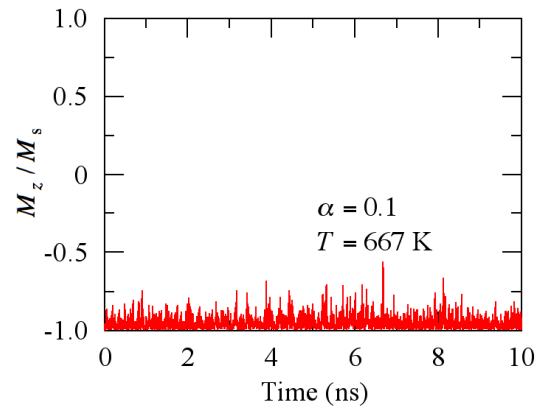


Fig. 8 Time dependence of magnetization z component M_z/M_s at 667 K (0.59 ns) for $\alpha = 0.1$ where $|H_w| = 10\text{ kOe}$ and $H_{\text{keff}} = 54\text{ kOe}$.

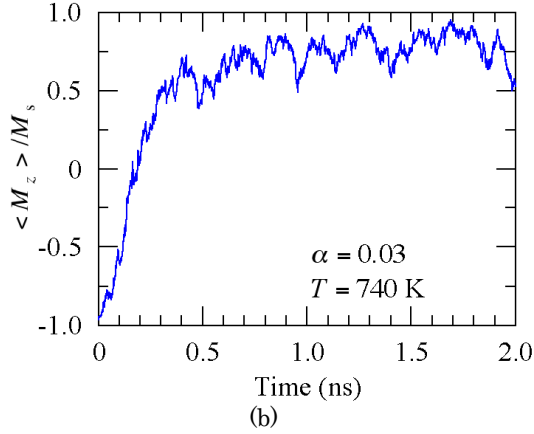
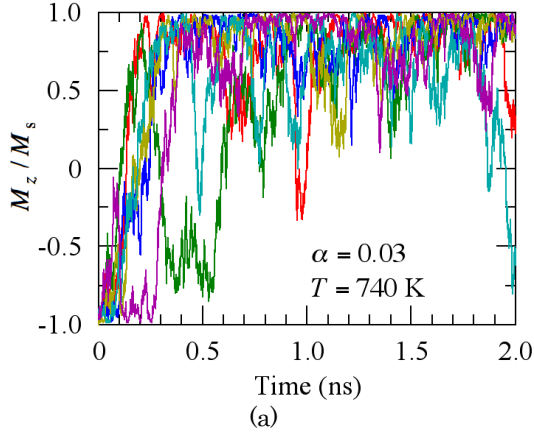


Fig. 9 (a) Time dependence of magnetization z component M_z/M_s calculated using six different random seeds at 740 K (0.070 ns) for $\alpha = 0.03$ where $|H_w| = 10$ kOe and $H_{\text{keff}} = 19$ kOe. (b) Mean magnetization $\langle M_z \rangle / M_s$ as a function of time.

667 K, the N_- value is about 10^{-3} times per nanosecond as shown in Fig. 6. This means that data can no longer be written, and this is confirmed in Fig. 8. The magnetization does not reverse and maintains its initial direction for 10 ns with this example. Therefore, to write data we need a magnetization reversal time much shorter than the field writing time of 1.27 ns.

When $\alpha = 0.03$, the $\langle M_z \rangle / M_s$ reversal time is 0.19 ns as shown in Fig. 9 (b), which is comparable to the $1/N_-(740 \text{ K})$ value of 0.24 ns. The $\langle M_z \rangle / M_s$ reversal time becomes longer than that for $\alpha = 0.1$.

For $\alpha = 0.01$, there is one case where no magnetization reversal occurs even within 2 ns for this example as shown in Fig. 10 (a). The $\langle M_z \rangle / M_s$ reversal time is long at 0.71 ns as shown in Fig. 10 (b), which is comparable to the $1/N_-(740 \text{ K})$ value of 0.72 ns. The $\langle M_z \rangle / M_s$ reversal time of 0.71 ns is too long for writing with reference to Fig. 6, namely, data can no longer be written. This is disadvantageous to writing.

The $1/N_-$ value is inversely proportional to α . The τ value is also inversely proportional to α as mentioned above. Furthermore, the H value in Eq. (17) includes the equivalent field for the energy of the thermal agitation, and the standard deviation of the equivalent

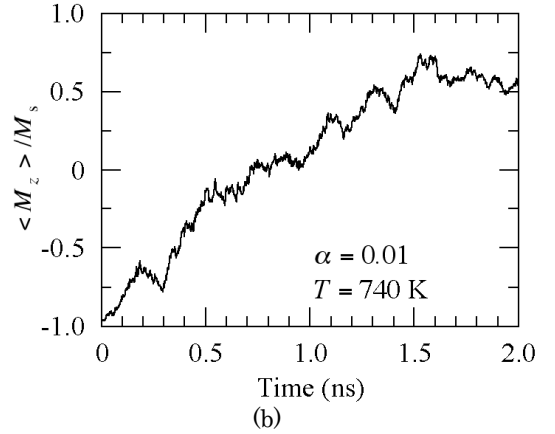
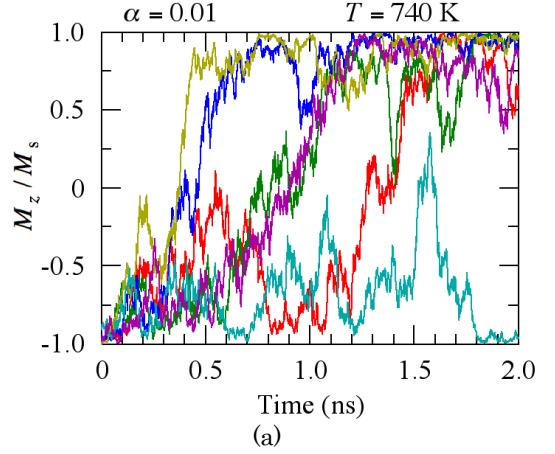


Fig. 10 (a) Time dependence of magnetization z component M_z/M_s calculated using six different random seeds at 740 K (0.070 ns) for $\alpha = 0.01$ where $|H_w| = 10$ kOe and $H_{\text{keff}} = 19$ kOe. (b) Mean magnetization $\langle M_z \rangle / M_s$ as a function of time.

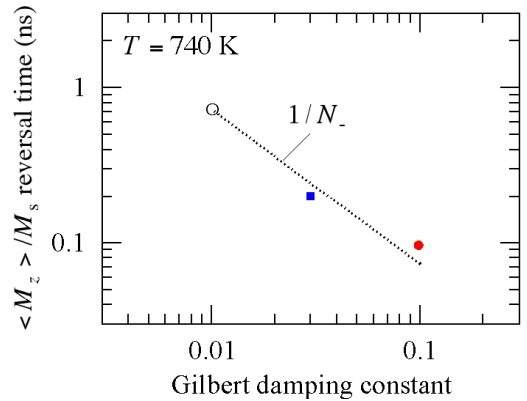


Fig. 11 Mean magnetization $\langle M_z \rangle / M_s$ reversal time as a function of Gilbert damping constant.

field is proportional to $\sqrt{\alpha}$. Figure 11 shows the $\langle M_z \rangle / M_s$ reversal time as a function of α . The $1/N_-$ value is also shown. The $\langle M_z \rangle / M_s$ reversal time and the $1/N_-$ value are almost the same and inversely proportional to α . Therefore, the $1/N_-$ value represents the stochastic magnetization reversal time under thermal agitation.

Many calculations are needed to find the mean value

in a micromagnetic simulation. However, in our stochastic calculation, the mean value can be found with one simple calculation of the N_{\pm} values, and therefore, the calculation time is short.

Overall, although the N_{+} value becomes small as shown in Fig. 4, a small α value is disadvantageous to writing as shown in Fig. 3 since the $1/N_{-}$ time becomes long.

4. Conclusions

We examined the influence of the damping constant α on writability in 4 Tbpsi shingled heated-dot magnetic recording, using our stochastic calculation. We confirmed the result of this calculation by employing a micromagnetic simulation.

The bit error rate was calculated and the result was analyzed using the mean magnetization reversal numbers per unit time N_{+} and N_{-} for magnetization reversal in the opposite direction to the recording direction and in the recording direction, respectively. The writing improved as the N_{+} and N_{-} values decreased and increased, respectively. Since the α value is considered to be smaller than 0.1, the N_{+} and N_{-} values decreased as the α value decreased.

The writing time where the N_{-} value is large is rather short compared with the field writing time. Therefore, the magnetization reversal time must be much shorter than the field writing time to write data. The $1/N_{-}$ value represents the stochastic magnetization reversal time under thermal agitation, and the $1/N_{-}$ value is inversely proportional to α . Although the N_{+} value becomes small, a small α value is disadvantageous to writing since the $1/N_{-}$ time becomes long. As a result, when the anisotropy constant is large, the bit error rate increases as the α value decreases.

The stochastic calculation results are consistent with those obtained with a micromagnetic simulation.

Acknowledgement We acknowledge the support of the Advanced Storage Research Consortium (ASRC), Japan.

References

- 1) S. H. Charap, P. -L. Lu, and Y. He: *IEEE Trans. Magn.*, **33**, 978 (1997).
- 2) F. Akagi, M. Mukoh, M. Mochizuki, J. Ushiyama, T. Matsumoto, and H. Miyamoto: *J. Magn. Magn. Mater.*, **324**, 309 (2012).
- 3) F. Akagi, Y. Sakamoto, and N. Matsushima: 2021 IEEE International Magnetic Conference (INTERMAG), 2100043 (2021). DOI: 10.1109/INTERMAG42984.2021.9580007
- 4) K. Maeda and F. Akagi: *T. Magn. Soc. Jpn.* (Special Issues) (in Japanese), **7**, 1 (2023).
- 5) T. Kobayashi, Y. Nakatani, and I. Tagawa: *J. Magn. Soc. Jpn.*, **48**, 81 (2024).
- 6) T. Kobayashi, Y. Nakatani, F. Inukai, K. Enomoto, and Y. Fujiwara: *J. Magn. Soc. Jpn.*, **41**, 52 (2017).
- 7) M. Mansuripur and M. F. Ruane: *IEEE Trans. Magn.*, **MAG-22**, 33 (1986).
- 8) J. -U. Thiele, K. R. Coffey, M. F. Toney, J. A. Hedstrom, and A. J. Kellock: *J. Appl. Phys.*, **91**, 6595 (2002).
- 9) T. Kobayashi and I. Tagawa: *J. Magn. Soc. Jpn.*, **48**, 40 (2024).
- 10) E. D. Boerner and H. N. Bertram: *IEEE Trans. Magn.*, **34**, 1678 (1998).
- 11) T. Kobayashi and I. Tagawa: *J. Magn. Soc. Jpn.*, **47**, 128 (2023).
- 12) T. Kobayashi, Y. Nakatani, and Y. Fujiwara: *J. Magn. Soc. Jpn.*, **42**, 110 (2018).
- 13) S. Uchiyama and M. Masuda: *Magnetic Materials* (in Japanese), p. 126 (Corona Publishing Co., Tokyo, 1980).
- 14) Fujitsu Release: *New Version of EXAMAG LLG Simulator*, <https://www.fujitsu.com/global/about/resources/news/press-releases/2015/0324-01.html> (2015).

Received Jul. 20, 2024; Accepted Oct. 4, 2024